Bioorganic & Medicinal Chemistry Letters 24 (2014) 4110–4113

Contents lists available at ScienceDirect

Bioorganic & Medicinal Chemistry Letters

journal homepage: www.elsevier.com/locate/bmcl

Discovery of pyrrolo-benzo-1,4-diazines as potent $Na_v1.7$ sodium channel blockers

Ginny D. Ho [a], Deen Tulshian [a], Ana Bercovici [a], Zheng Tan [a], Jennifer Hanisak [a], Stephanie Brumfield [a], Julius Matasi [a], Charles R. Heap [b], William G. Earley [b], Brandy Courneya [b], R. Jason Herr [b], Xiaoping Zhou [c], Terry Bridal [d], Diane Rindgen [e], Steve Sorota [d], Shu-Wei Yang [a,*]

[a] Discovery Chemistry, Merck Research Laboratory, Kenilworth, NJ 07033, United States
[b] Department of Medicinal Chemistry, AMRI Global, Albany, NY 12203, United States
[c] In Vivo Pharmacology Group, Merck Research Laboratory, Kenilworth, NJ 07033, United States
[d] Cardiorenal Group, Merck Research Laboratory, Kenilworth, NJ 07033, United States
[e] Pharmacokinetics, Pharmacodynamics and Drug Metabolism, Merck Research Laboratory, Kenilworth, NJ 07033, United States

ARTICLE INFO

Article history:
Received 22 April 2014
Revised 17 July 2014
Accepted 21 July 2014
Available online 29 July 2014

Keywords:
Nav1.7
Nav1.5
Pain
Sodium channel blockers
Pyrrolo-benzo-1,4-diazine

ABSTRACT

A series of pyrrolo-benzo-1,4-diazine analogs have been synthesized and displayed potent $Na_v1.7$ inhibitory activity and moderate selectivity over $Na_v1.5$. The syntheses, structure–activity relationships, and selected pharmacokinetic data of these analogs are described. Compound **41** displayed anti-nociceptive efficacy in the rat CFA pain model at 100 mpk oral dosing.

Voltage-gated sodium channels (VGSCs), a family of nine sodium channel subtypes, generate and proliferate action potentials in excitable cells, and are crucial for muscle and nerve function.[1] Although most compounds identified as sodium channel blockers do not display selectivity against all channel subtypes, a few blockers have been shown to produce sufficient therapeutic selectivity and window for the treatment of action potential maladies such as epilepsy (phenytoin), pain (lidocaine), and certain cardiac arrhythmia (mexiletine).

$Na_v1.7$ is a VGSC that is highly expressed in nociceptive neurons and sympathetic ganglia.[2] It plays a critical role in the generation and conduction of electrical signaling in small and medium-diameter sensory afferent nerves.[3] Knockout mice lacking $Na_v1.7$ in $Na_v1.8$ expressing neurons displayed reduced pain response to mechanical or inflammatory pain.[4] Humans lacking $Na_v1.7$ exhibit a profound loss of all pain sensation.[5] Consistent with the human phenotype, a more complete loss of pain sensation was observed in a pan-neuronal $Na_v1.7$ knockout mouse.[4] In contrast to the human and mouse knockout phenotype gain of function mutations in $Na_v1.7$ causes pain syndromes in humans, either primary erythromelalgia or paroxysmal extreme pain syndrome.[6,7] On balance these observations suggest that $Na_v1.7$ provides an excellent therapeutic target for pain relief.

In our $Na_v1.7$ program we screened our compound collection using veratridine-modified human $Na_v1.7$ and $Na_v1.5$ channels and a voltage-sensitive dye in FLIPR assays. $Na_v1.5$ channel is the major VGSC in the heart. Block of Nav1.5 is undesirable because it is responsible for the cardiac action potential initiation and conduction. The project goal was to identify $Na_v1.7$ blockers with reasonable selectivity against $Na_v1.5$ channels in vitro, and most importantly in vivo. During high-throughput screening (HTS) of our compound collection, some analogs with the pyrrolo-benzo-1,4-diazine skeleton were identified to display $Na_v1.7$ inhibitory activity and modest selectivity against human $Na_v1.5$. Compound **1**, the initial lead, displayed potent $Na_v1.7$ inhibitory activity (IC_{50} 160 nM) with ~50-fold selectivity over $Na_v1.5$ in the FLIPR screen, shown in Figure 1. This apparent selectivity decreased to ~10-fold when whole cell sodium currents were measured in manual voltage clamp (VC) with 50 ms depolarizations at 10 Hz from a holding potential of −120 mV. However **1** did not exhibit high

* Corresponding author. Tel.: +1 908 740 2589.
E-mail address: shu-wei.yang@merck.com (S.-W. Yang).

http://dx.doi.org/10.1016/j.bmcl.2014.07.060
0960-894X/

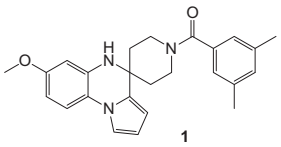

NaV1.7 IC_{50}: 160 nM
NaV1.5 IC_{50}: 8092 nM
rat-AUC_{6h}: 788 nM.h

Figure 1. Initial HTS lead compound **1**, and its biological data.

plasma exposure in rat based on area under curve (AUC) data (AUC_{6h}: 788 nM h).

Our strategy was to quickly identify $Na_v1.7$ blockers which exhibited in vivo efficacy for proof of concept. Therefore achieving high oral plasma exposure was considered as an important goal. Rat pharmacokinetic (PK) AUC values of the active compounds were obtained to guide the compound selection for further in vivo study. In this communication, we describe syntheses and structure activity relationships (SAR) of the pyrrolo-benzo-1,4-diazine series versus $Na_v1.5$, $Na_v1.7$, and plasma exposure. The PK and in vivo data of selected compounds are described.

The synthetic route to the key intermediate **5** is summarized in Scheme 1. The reaction of nitro-aniline **2** with 2,5-dimethoxytetrahydrofuran (2,5-DMTHF) in acetic acid, followed by reduction of the nitro group using $BiCl_3$–$NaBH_4$ yielded pyrrolo-aniline intermediates **3**.[8] The pyrrole intermediates (**3**) were then cyclized with piperidin-4-one or N-substituted piperidin-4-one derivatives to form 5′*H*-spiro[piperidine-4,4′-pyrrolo[1,2-*a*]quinoxaline] cores (**4**–**7**). Intermediates **5** were the major intermediates for further diverse modification. Cyclization of pyrrolo-anilines **3** and *N*-substituted piperidin-4-one derivatives allowed us to directly obtain certain desired targets, such as carbamates (**4**), amides (**7**), and amines (**6**). However this strategy showed restriction due to limited commercially available substituted piperidin-4-ones. The late stage intermediates **5** were the subjects for versatile and feasible structure modification. In general the yields of the cyclization (reaction c in Scheme 1) to form **4**–**7** were excellent (>80%).

Conversion of intermediates **5** to sulfonamides, N-substituted amines, amides, and ureas is shown in Scheme 2. Standard procedures were used to prepare these intermediates. The commercially

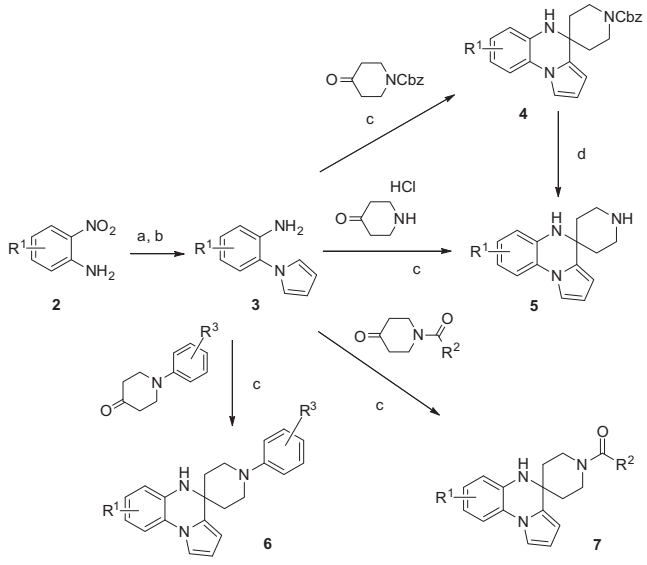

Scheme 1. Reagents and conditions: (a) 2,5-DMTHF, AcOH, reflux (~70–90%); (b) $BiCl_3$, $NaBH_4$, EtOH (~50–80%); (c) cat. maleic acid, EtOH, 80 °C (>80%); (d) H_2 (1 atm), Pd/C, EtOH (>90%).

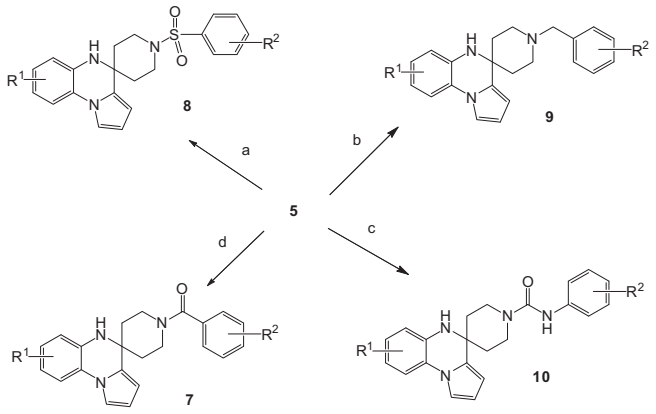

Scheme 2. Reagents and conditions: (a) R^2-Ph-SO_2Cl, Et_3N, CH_2Cl_2, rt (~30–50%); (b) R^2-benzyl bromide, DIPEA, DMF (~60–70%); (c) R^2-PhNCO, Et_3N, CH_3CN, 0 °C to rt (~50–60%); (d) R^2CO_2H, EDC, HOAt, DMAP, DIPEA, CH_2Cl_2 (~50–85%).

available sulfonyl chlorides, isocyanates, and substituted benzyl bromides were reacted with **5** under basic conditions to form sulfonamides (**8**), ureas (**10**), and benzyl amines (**9**), respectively. Substituted amides were prepared under EDC–HOAt coupling condition. The amides shown in Tables 1, 2, 4 and 5 were prepared from intermediates **5** according to this condition.

Target compounds were tested for their inhibitory activities at the cloned human VGSCs ($Na_v1.7$ or $Na_v1.5$) expressed in HEK 293 cells by measuring fluorescence from a membrane potential dye. After 60 min of compound and dye loading, cell depolarization was evoked on the FLIPR by the addition of veratridine. Maximum veratridine-induced increase in fluorescence intensity from baseline was used to plot concentration-effect curves and generate IC_{50} values. The rat PK assay was carried out with oral dosing at 10 mpk, and the AUC values were measured over a 0–6 h duration.

The initial SAR study focused on analogs without substitution on the left-hand-side (LHS) phenyl ring and with varying substitution on the right-hand-side (RHS) phenyl ring (Table 1). Compounds **11** and **12** with no or cyano substitution, respectively, on the RHS phenyl ring did not show activity up to 3 μM. Compound **13** with 3-*N*,*N*-dimethyl substitution displayed reasonable $Na_v1.7$ inhibitory activity (IC_{50} 381 nM), and poor selectivity against $Na_v1.5$ (~11-fold). The 3,5-di-methyl substitution (**14**) however greatly improved $Na_v1.7$ inhibitory activity (IC_{50} 47 nM) and selectivity over $Na_v1.5$ (379-fold). Unfortunately **14** did not show detectable plasma exposure in the rat PK study (AUC_{6h} 0 nM h). Although 4-cyano analog **12** was inactive up to 3 μM in the $Na_v1.7$ FLIPR assay, it showed some plasma exposure (AUC_{6h} 1011 nM h) in the rat PK study. Hence additional analogs with 4-cyano-phenyl moiety were prepared for further SAR study.

Table 1
SAR of the analogs with the RHS substitution

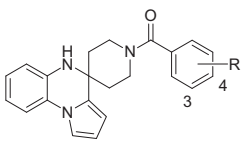

	R	$Na_v1.7$ IC_{50}[a] (nM)	$Na_v1.5$ IC_{50}[a] (nM)	AUC_{6h} (nM h)
11	H	>3000	ND	ND
12	4-CN	>3000	ND	1011
13	3-N(CH_3)$_2$	381	4384	633
14	3,5-Di-(CH_3)$_2$	47	17810	0

[a] IC_{50} represent single determinations performed with four replicates per concentration point.

Table 2
SAR of the 7- or 8-substituted analogs

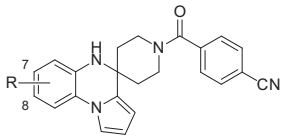

	R	$Na_v1.7$ IC_{50}[a] (nM)	$Na_v1.5$ IC_{50}[a] (nM)	AUC_{6h} (nM h)
15	7-OCH_3	613	13770	51081
16	7-OCF_3	81	1452	11658
17	7-CF_3	311	4871	15202
18	7-Cl	404	8289	2897
19	8-F	478	9291	11982
20	8-Cl	563	8144	26066
21	8-Br	344	9174	23416

[a] IC_{50} represent single determinations performed with four replicates per concentration point.

Table 3
SAR of the analogs with different linkers

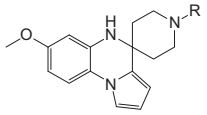

	R	$Na_v1.7$ IC_{50}[a] (nM)	$Na_v1.5$ IC_{50}[a] (nM)	AUC_{6h} (nM h)
22	CO_2-Bn	1500	6882	13108
23	Bn	17	455	370
24	4-CN-Bn	562	4577	ND
25	3-CN-Ph	9279	12875	ND
26	CONH-(4-CN-Ph)	8732	>30000	ND
27	SO_2-(4-CN-Ph)	6966	ND	ND

[a] IC_{50} represent single determinations performed with four replicates per concentration point.

Substitution on the LHS phenyl ring was carried out mainly on 7- or 8-position due to their potential of being metabolized. A series of compounds with different substitutions on C-7 and C-8 were prepared. The data of selected compounds (**15**–**21**) are summarized in Table 2. These compounds possessed similar inhibitory and selectivity profiles ($Na_v1.7$/$Na_v1.5$: between 15 and 27 folds). Compound **16** with 7-OCF_3 substitution displayed most potent $Na_v1.7$ blocking activity (IC_{50} 81 nM). The strategy of blocking potential metabolic spots was very successful. All these compounds showed moderate to great plasma exposure in the rat PK study with AUC_{6h} values between 2.9 and 51 μM h. Among them, the 7-methoxyl analog (**15**) exhibited the highest plasma exposure in the rat oral PK study (AUC_{6h} 51081 nM h). In addition a few 6- or 9-substituted analogs were prepared. However, all of them showed poor selectivity over $Na_v1.5$ (<6-fold, data not shown), and were not further explored.

In parallel the linkers between the core and the RHS phenyl ring were examined. The data of some selected compounds (**22**–**27**) are listed in Table 3. Among these representatives, carbamate **22**, urea **26**, sulfonamide **27**, and *N*-phenyl analog **25** all showed poor $Na_v1.7$ activity (>1500 nM) and selectivity over $Na_v1.5$ (<5-fold). The benzyl analog **23** showed excellent activity in the $Na_v1.7$ FLIPR assay (IC_{50} 17 nM), but failed to display adequate oral plasma exposure (AUC_{6h} 370 nM h). From this SAR information we further focused on compounds with the amide linkage, the LHS 7-OCH_3 substitution, and varying substitution on the RHS phenyl ring.

The data of ten selected mono-substituted analogs (**28**–**37**) are summarized in Table 4. Substitution with 2-OCH_3 (**28**) or 2-Br (**29**)

Table 4
SAR of the RHS mono-substituted analogs

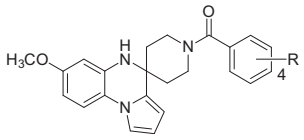

	R	$Na_v1.7$ IC_{50}[a] (nM)	$Na_v1.5$ IC_{50}[a] (nM)	AUC_{6h} (nM h)
28	2-OCH_3	436	4891	0
29	2-Br	414	7601	ND
30	3-OCH_3	280	4325	0
31	3-CH_3	321	7172	0
32	3-Cl	48	4418	0
33	3-CN	201	9716	783
34	4-OCH_3	437	8033	91493
35	4-CH_3	312	6943	17199
36	4-Cl	94	3949	1960
37	4-$N(CH_3)_2$	56	947	9436

[a] IC_{50} represent single determinations performed with four replicates per concentration point.

Table 5
SAR of the RHS di-substituted analogs

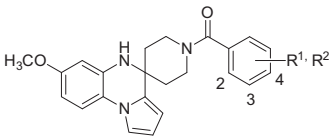

	R^1,R^2	$Na_v1.7$ IC_{50}[a] (nM)	$Na_v1.5$ IC_{50}[a] (nM)	AUC_{6h} (nM h)
38	3-OCH_3, 4-CN	439	7240	26641
39	3-Cl, 4-$N(CH_3)_2$	9	572	1271
40	3-Cl, 4-OCH_3	37	934	6809
41	3-$N(CH_3)_2$, 4-OCH_3	9	351	20271
42	3-OCH_3, 4-$N(CH_3)_2$	87	1329	ND

[a] IC_{50} represent single determinations performed with four replicates per concentration point.

did not improve inhibitory activity and selectivity over $Na_v1.5$, and failed to show detectable plasma exposure in the rat PK study. Among four 3-substituted analogs (**30**–**33**), 3-chloro substitution (**32**) improved $Na_v1.7$ inhibitory activity (IC_{50} 48 nM) and selectivity over $Na_v1.5$ (92-fold). However, only the 3-cyano analog (**33**) displayed some oral plasma exposure (AUC_{6h} 783 nM h), and **30**–**32** were not detectable in the rat plasma after oral dosing at 10 mpk. Compared to 3-substituted analogs, 4-substituted analogs (**34**–**37**) displayed similar $Na_v1.7$ and $Na_v1.5$ profiles, whereas the plasma exposures of these compounds significantly improved. Compound **34** with 4-OCH_3 substitution exhibited outstanding AUC_{6h} value (~91 μM h). From these SAR data, 4-position of the RHS phenyl ring appeared to be the metabolic hot spot in the amide series. Blocking this position greatly enhanced the oral PK plasma exposure. Although **34** showed great metabolic stability, the potency and the selectivity could be further improved. Hence we shifted our focus to the bi-substituted analogs.

Selected bi-substituted analogs (**38**–**42**) and their data are summarized in Table 5. To maintain good PK profile, all selected compounds possessed 4-substitution on the RHS phenyl ring. Among them, two *N*,*N*-dimethylamino analogs (**39** and **41**) showed highly potent $Na_v1.7$ inhibitory activity (IC_{50} 9 nM) and moderate selectivity over $Na_v1.5$ (63- and 39-fold, respectively). Compound **41** with 4-methoxy and 5-*N*,*N*-dimethylamino substitutions pos-

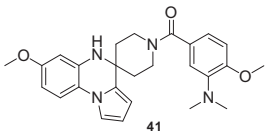

41

Nav1.7 IC_{50} 9 nM (FLIPR)
Nav1.5 IC_{50} 572 nM (FLIPR)
Nav1.7 IC_{50} 331 nM (VC)
Nav1.5 IC_{50} 10485 nM (VC)
hERG (iw): 3% inh @1 uM
14% inh. @ 10 uM
Rat AUC_{6h}: 20271 nM.h
brain conc.$_{6h}$: 257 ng/g

Figure 2. Optimized compound **41**, and its in vitro and PK data.

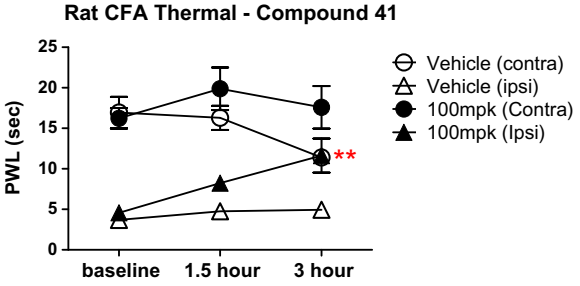

Figure 3. CFA inflammatory pain responses at 1.5 and 3 h for compound **41** at 100 mpk PO (▲, ipsilateral and ●, contralateral) versus vehicle (△, ipsilateral and ○, contralateral) in the rat CFA model.[9]

sessed superior rat plasma exposure (AUC_{6h} ~20 μM h) compared to **39** (1271 nM h), and was selected for further in vitro and in vivo studies.

Compound **41** was further investigated in the $Na_v1.5$ and $Na_v1.7$ voltage clamp (VC) and the Human Ether-a-go-go Related Gene (hERG) assays (Fig. 2). Standard ruptured whole cell patch clamp techniques were used to measure direct Na channel blocking activity. The desired compound should show low effect in these undesired targets, such as hERG, a potassium ion channel which regulates heart rhythm. Compound **41** showed IC_{50} 331 nM in the $Na_v1.7$ VC assay, and ~32-fold selectivity over $Na_v1.5$ (VC). It did not show a high percentage inhibition in the hERG assay (14% at 10 μM).

Compound **41** was evaluated for efficacy in the in vivo rat Complete Freund's Adjuvant (CFA) induced inflammatory pain model. The pain inducing substance was injected into one of the hind paws of the animal to induce an inflammatory response. Thermal hyperalgesia was then measured two days after CFA treatment based on paw withdrawal latency (PWL) to determine the pain relief ability of $Na_v1.7$ blocker **41** versus control at 0 h, 1.5 h and 3 h. The assay was validated with morphine, naproxen and mexiletine (oral dosing). As expected, morphine (5 mpk) had effects on both the ipsilateral and contralateral paws. Mexiletine (60 mpk) had significant effects on the contralateral but not the ipsilateral paw. Naproxen (30 mpk) only affected the ipsilateral paw. Compared to the vehicle, **41** significantly increased PWL at 3 h following oral dosing at 100 mpk. Compound **41** displayed excellent oral PK profile with 100% bioavailability in 24 h study (Table 6). Average plasma concentrations of **41** at 3.5 h post dosing within the CFA thermal study were 47 μM (rat plasma protein binding 98.4%). The results demonstrated that $Na_v1.7$ blocker **41** was able to reduce pain sensation.

Table 6
Full rat PK data of **41**

	iv	po
Number of animals[a]	3	3
Dose (mg/kg)	3	10
$AUC_{(0-24)}$ (μM h)	17.4	65.9
Terminal half-life (h)	2.9	
Bioavailability (%)		100
Mean residence time (MRT) (h)	3.0	4.7
C_{max} (μM); T_{max} (h)		9.3; 1.3
Clearance (mL/min/kg)	6.5	
Vd(ss) (L/kg)	1.2	

[a] Male CD rats were used in this study.

In conclusion, a novel series of potent $Na_v1.7$ inhibitors with moderate selectivity over $Na_v1.5$ based on the pyrrolo-benzo-1,4-diazine scaffold were discovered. The initial SAR studies based on $Na_v1.7$ blocking, selectivity over $Na_v1.5$, and plasma exposure (PK AUC_{6h}) versus structures were established. In particular, the 7- or 8-substitution on the LHS phenyl ring was very important for the molecule to maintain good metabolic stability, as well as 4-substitution on the RHS phenyl ring. To quickly achieve proof of concept, we selected **41** with potent $Na_v1.7$ inhibitory activity, moderate selectivity over $Na_v1.5$, and excellent PK profile for further in vivo study. Compound **41** exhibited anti-nociceptive efficacy in the rat CFA pain model at 100 mpk oral dosing. Further improvements to this scaffold should furnish an improved $Na_v1.7$ inhibitor, which may be useful as an anti-nociceptive agent.

Acknowledgments

The authors wish to acknowledge Drs. William Greenlee and George Njoroge for providing the insight for this program, Dr. Tze-Ming Chan and his group for structure confirmation of some analogs, and the DMPK group for acquiring pharmacokinetic data.

References and Notes

1. Clare, J. J.; Tate, S. N.; Nobbs, M.; Romanos, M. A. *Drug Discovery Today* **2000**, *5*, 506.
2. (a) Klugbauer, N.; Lacinova, L.; Flockerzi, V.; Hofmann, F. *EMBO J.* **1995**, *1084*, 14; (b) Plummer, N. W.; Meisler, M. H. *Genomics* **1999**, *57*, 323.
3. (a) Raymond, C. K.; Castle, J.; Garrett-Engele, P.; Armour, C. D.; Kan, Z.; Tsinoremas, N.; Johnson, J. M. *J. Biol. Chem.* **2004**, *279*, 46234; (b) Rush, A. M.; Dib-Hajj, S. D.; Liu, S.; Cummins, T. R.; Black, J. A.; Waxman, S. G. *Proc. Natl. Acad. Sci. U.S.A.* **2006**, *103*, 8245.
4. (a) Nassar, M. A.; Stirling, L. C.; Forlani, G.; Baker, M. D.; Matthews, E. A.; Dickenson, A. H.; Wood, J. N. *Proc. Natl. Acad. Sci. U.S.A.* **2004**, *101*, 12706; (b) Minett, M. S.; Nassar, M. A.; Clark, A. K.; Passmore, G.; Dickenson, A. H.; Wang, F.; Malcangio, M.; Wood, J. N. *Nat. Commun.* **2012**, *3*, 791.
5. Cox, J. J.; Reimann, F.; Nicholas, A. K.; Thornton, G.; Roberts, E.; Springell, K.; Karbani, G.; Jafri, H.; Mannan, J.; Raashid, Y.; Al-Gazali, L.; Hamamy, H.; Valente, E. M.; Gorman, S.; Williams, R.; McHale, D. P.; Wood, J. N.; Gribble, F. M.; Woods, C. G. *Nature* **2006**, *444*, 894.
6. Drenth, J. P.; Michiels, J. J. *Int. J. Dermatol.* **1994**, *33*, 393.
7. Dib-Hajj, S. D.; Cummins, T. R.; Black, J. A.; Waxman, S. G. *Trends Neurosci.* **2007**, *30*, 555.
8. Guillon, J.; Grellier, P.; Labaied, M.; Sonnet, P.; Léger, J. M.; Déprez-Poulain, R.; Forfar-Bares, I.; Dallemagne, P.; Lemaître, N.; Péhourcq, F.; Rochette, J.; Sergheraert, C.; Jarry, C. *J. Med. Chem.* **2004**, *1997*, 47.
9. In Figure 3. One hind paw of rat subjects (6 rats per group) was treated with Freud's Adjuvant to induce an inflammatory pain response. With only vehicle (Δ, ipsilateral) treatment, PWL remained the same during the 3 h period under thermal conditions. With **41** (100 mpk po), PWL significantly increased at 3 h (▲ ipsilateral). Therma PWL in the non-inflammed hind paw was also measured, first with only vehicle administration (○ contralateral). Compound **41** (100 mpk oral dosing) displayed increased thermal PWL in the contralateral paw (●) at 3 h post dosing. Male CD rats (Charles River Laboratories version of Sprague Dawley) were used for both PK and PD studies.